Liquid Crystals
Publication details, including instructions for authors and subscription information:
http://www.informaworld.com/smpp/title~content=t713926090

On the dynamics of ferro- and antiferro-electric liquid crystals

Masahiro Nakagawa[a]
[a] Department of Electrical Engineering, Faculty of Engineering, Nagaoka University of Technology, Niigata, Japan

To cite this Article Nakagawa, Masahiro(1993) 'On the dynamics of ferro- and antiferro-electric liquid crystals', Liquid Crystals, 14: 6, 1763 — 1784
To link to this Article: DOI: 10.1080/02678299308027714
URL: http://dx.doi.org/10.1080/02678299308027714

LIQUID CRYSTALS, 1993, VOL. 14, NO. 6, 1763–1784

On the dynamics of ferro- and antiferro-electric liquid crystals

by MASAHIRO NAKAGAWA
Department of Electrical Engineering, Faculty of Engineering, Nagaoka University of Technology, Kamitomioka 1603, Nagaoka, Niigata 940-21, Japan

In this work, a set of Landau–Ginzburg equations to investigate the dynamic properties of ferro- and antiferro-electric smectic phases is formulated on the basis of the elastic continuum theory of compressible smectics. In the present framework, the polarization electric field is consistently taken into account through the Poisson equation as seen in our previous work. As a practical application, a few numerical results are presented for the surface-stabilized geometry with inclined and chevron layer structures. An asymmetric bistable switching is found to be achieved in the chevron layer structure under an alternating external field. In an inclined layer structure, however, a symmetric switching is found to be possible. In addition, it is first presented from a theoretical standpoint that the compressible smectic layer structure may be drastically deformed in the chevron and inclined layer structures with a sufficiently large external field.

1. Introduction

Recently ferroelectric and the antiferroelectric liquid crystals have been actively investigated from the experimental and also theoretical point of views, because of their attractive potentiality for application to fast electro-optic devices [1–5]. According to earlier pioneering work in this field, the material properties of smectics have certainly blossomed, whereas most material properties of smectics have been accompanied by many open questions because of the difficulty in obtaining experimentally large monodomain samples. Also the elastic properties of smectics have not been well clarified from a theoretical point of view.

From the previously mentioned point of view, the elastic free energy of the S_C phase was first formulated by the Orsay group in terms of an axial vector in a local coordinate system [6]. Later Rapini expressed it in a vector notation in the laboratory frame for practical applications of continuum theory [7]. The chiral energy was also later included in the elastic free energy for the S_C^* phase as seen in de Gennes' book [8]. Another vector expression of the S_C^* phase was recently reported by Dahl and Lagerwall [9]. Recently, the present author put forward a generalized elastic free energy for compressible smectics in order to account for the layer compression or dilation [10] and analysed the chevron layer structure [11–13] which has been observed in high resolution X-ray experiments [14–16]. The effect of the electric field in the chevron layer structure was investigated for static deformations [12, 13]. It was found therein that the electric field parallel to the spontaneous polarization vector $\mathbf{P}_S$ tends to make the layer tilt angle small in a chevron layer structure, whereas the electric field opposite to $\mathbf{P}_S$ acts to make it large [12]. In addition, it was also concluded that the **c** director orientation can be easily distorted in comparison with the layer structure [13]. In previous work, while the static deformation of the S_C^* was investigated analytically, as well as numerically, to clarify the elastic properties of compressible

0267-8292/93 $10.00

smectics, the dynamics of compressible smectics has not been treated yet. Therefore it is expected that a theoretical study of the dynamical properties of smectics may shed new light on the understanding of smectics. In this respect, a hydrodynamic theory of incompressible S_C liquid crystals has been proposed by Leslie, Stewart and Nakagawa [17]. However, there has been no report of any hydrodynamic theory for a compressible S_C^* phase as far as we are aware. Therefore we shall resort at this stage to a somewhat phenomenological approach, instead of using the previous framework [17].

In the present work, we shall formulate a basic set of time dependent differential equations to investigate the dynamic property of compressible smectics. It seems to be important to confirm the possibility of bistable switching, which is an attractive characteristic from an application point of view. In this work, a weak anchoring for the **c** director orientation on the bounding surfaces is assumed to simulate a dynamical bistable switching. In § 2, a theoretical formulation will be presented on the basis of the elastic free energy of compressible smectics [10, 13]. Then a few numerical results will be provided in § 3 to show a possible electric field effect on the smectic layer structure. Finally § 4 will be devoted to some concluding remarks on the presently found layer dynamics in smectic phases.

2. Theory

In compressible smectics [10, 13, 18], the elastic free energy may be simply written as

$$F=\frac{A}{2}(\nabla\cdot\mathbf{a})^2+\frac{B}{2}\sum_i\{(\nabla\cdot\mathbf{c}_i)^2+(\nabla\times\mathbf{c}_i)^2\}-C\sum_i(\nabla\cdot\mathbf{a})(\nabla\cdot\mathbf{c}_i)-D\sum_i(\mathbf{c}_i\cdot\nabla\times\mathbf{c}_i)$$
$$+\frac{L}{2}(|\mathbf{a}|-|\mathbf{a}_0|)^2+\sum_i\mathbf{P}_i\cdot\nabla\varphi-\tfrac{1}{2}\nabla\varphi\cdot\underline{\varepsilon}\cdot\nabla\varphi+K_p\mathbf{P}_o\cdot\mathbf{P}_e \quad (1)$$

where **a** is the wave vector along the layer normal whose magnitude is defined by

$$|\mathbf{a}|=\frac{d_A}{d(\mathbf{r},t)} \quad (2)$$

$\mathbf{c}_i$ is the **c** director in the ith layer, the subscript i ranges over the odd-numbered layers (abbreviated as o) and the even-numbered ones (abbreviated as e), A, B and C are the elastic constants for the layer distortion, the **c** director deformation and a coupling constant between them, D is a chiral elastic constant, L is an elastic modulus for the layer compression, φ is the electrostatic potential, $\underline{\varepsilon}$ denotes the dielectric tensor which may depend on **a** and $\mathbf{c}_i$ ($i=$ o and e), $|\mathbf{a}_0|$ is a constant regarded as an equilibrium value of $|\mathbf{a}|$, and K_p is a coupling constant between the adjacent dipoles in the odd-numbered layers and the even-numbered ones [18], i.e. between $\mathbf{P}_o$ and $\mathbf{P}_e$, which takes positive or negative value for the antiferroelectric or the ferroelectric states, respectively. For a special case such that **a** and $\mathbf{c}_i$ ($i=$ o and e) are spatially constant, the present free energy density (see equation (1)) may be reduced to that introduced in previous work [18]. $\mathbf{P}_o$ and $\mathbf{P}_e$ are assumed to be parallel to $\mathbf{a}\times\mathbf{c}_o$ and $\mathbf{a}\times\mathbf{c}_e$, respectively, as was earlier modelled by Chandani *et al.* [19]. For an incompressible smectic, one has to put $\mathbf{a}\cdot\mathbf{a}=1$, in addition to $\nabla\times\mathbf{a}=0$ and $\mathbf{c}_i\cdot\mathbf{c}_i=1$ ($i=$ o and e). The general expression of the elastic free energy for such a special case was previously formulated in a vector expression [20] and also in a tensor expression [21].

Let us assume one dimensional distortion along the y axis and put $\mathbf{a}$, $\mathbf{c}_i$, and $\mathbf{P}_i$ into the following

$$\mathbf{a}(y,t)=(0,a_y,a_z) \tag{3 a}$$
$$=(0,\tan\theta,1)$$

$$\mathbf{c}_i(y,t)=(\cos\phi_i,\cos\theta\sin\phi_i,-\sin\theta\sin\phi_i), \tag{3 b}$$

$$\mathbf{P}_i(y,t)=(-P_s\cdot\sin\phi_i,\ P_s\cdot\cos\theta\cos\phi_i,\ -P_s\cdot\sin\theta\cos\phi_i), \tag{3 c}$$

which are consistent with $\nabla\times\mathbf{a}=0$, $\mathbf{a}\cdot\mathbf{c}_i=0$, $\mathbf{c}_i\cdot\mathbf{c}_i=1$, and $\mathbf{P}_i=P_S(\mathbf{a}\times\mathbf{c}_i)/|\mathbf{a}|$. Here a_z was put into a constant without loss of generality, because of $\nabla\times\mathbf{a}=0$, and may be set to 1 at the boundaries due to the assumption such that the smectic molecules at the boundaries retain the same layer spacing as in the S_A phase with $a_y=0$ and $|\mathbf{a}|=1$, or $a_z=1$ (see equation (2)). Consequently a_y was put into $\tan\theta\ (=a_y/a_z)$ as in equation (3 a). It should be noted here that the chevron layer structure may be accompanied by layer compression $|\mathbf{a}|>|\mathbf{a}_0|\ (=\sec\theta_0>1)$, as well as dilation $|\mathbf{a}|<|\mathbf{a}_0|$. Substituting equations (3 a–c) into equation (1), one eventually has the following expression:

$$\begin{aligned}F=&\frac{A}{2}\sec^4\theta\left(\frac{\partial\theta}{\partial y}\right)^2+\frac{B}{2}\sum_i\left\{\sin^2\phi_i\left(\frac{\partial\theta}{\partial y}\right)^2+\left(\frac{\partial\phi_i}{\partial y}\right)^2\right\}\\&-C\sec^2\theta\left(\frac{\partial\theta}{\partial y}\right)\sum_i\left\{-\sin\theta\sin\phi_i\left(\frac{\partial\theta}{\partial y}\right)+\cos\theta\cos\phi_i\left(\frac{\partial\phi_i}{\partial y}\right)\right\}\\&-D\sum_i\left\{-\cos\phi_i\left(\frac{\partial(\sin\theta\sin\phi_i)}{\partial y}\right)+\sin\theta\sin\phi_i\left(\frac{\partial(\cos\phi_i)}{\partial y}\right)\right\}\\&+\mathbf{P}_S\left(\frac{\partial\varphi}{\partial y}\right)\sum_i\cos\theta\cos\phi_i+\frac{L}{2}(\sec^2\theta-\sec^2\theta_0)^2+\mathbf{K}_p\mathbf{P}_S^2\cos(\phi_0-\phi_e)-\frac{\varepsilon_{yy}}{2}\left(\frac{\partial\varphi}{\partial y}\right)^2,\end{aligned} \tag{4}$$

where $\mathbf{P}_S$ is defined by $|\mathbf{P}_i|$, ε_{yy} is a diagonal component of the dielectric tensor ε along the y axis and may depend on θ and ϕ_i in general, and θ_0 is an apparent molecular tilt angle defined by

$$\theta_0=\cos^{-1}\left(\frac{d_C}{d_A}\right); \tag{5}$$

here d_C and d_A are the layer spacing in the S_C^* (or S_{CA}^*) and in the S_A phases, respectively since $|\mathbf{a}_0|=d_A/d_C$ and $d_C=d_A\cos\theta_0$. In equation (4) the term proportional to $B\sin^2\phi_i(\partial\theta/\partial y)^2$ can be regarded as an anchoring energy near the chevron tip with a relatively large value of $(\partial\theta/\partial y)^2$. Hence one may deduce that the steeper the chevron becomes, the stronger the apparent anchoring force becomes.

Now the surface anchoring free energies at the boundaries are assumed to depend on only $\mathbf{c}_i$ or ϕ_i, and to be given by [21]

$$f_s^0(\phi_i)=-\frac{g}{2}\left[\exp\left\{-\sigma\sin^2\left(\frac{(\phi_i-\phi_0^0)}{2}\right)\right\}+\exp\left\{-\sigma\cos^2\left(\frac{(\phi_i+\phi_0^0)}{2}\right)\right\}\right], \tag{6 a}$$

$$f_s^d(\phi_i)=-\frac{g}{2}\left[\exp\left\{-\sigma\sin^2\left(\frac{(\phi_i-\phi_0^d)}{2}\right)\right\}+\exp\left\{-\sigma\cos^2\left(\frac{(\phi_i+\phi_0^d)}{2}\right)\right\}\right], \tag{6 b}$$

for $y=0$ and $y=d$, respectively, where $g(>0)$, $\sigma(>0)$, and ϕ_0 are the anchoring strength, the steepness of the anchoring potential well, and a preferred azimuthal angle of $\mathbf{c}_i$ at the boundary, respectively.

Thus the total elastic free energy per unit area F can be derived as

$$\mathrm{F}\{\theta, \phi_i, \varphi\} = \int_0^d dy \left\{ F(\theta, \phi_i, \varphi) + \sum_i f_s^0(\phi_i)\delta(y) + \sum_i f_s^d(\phi_i)\delta(y-d) \right\}, \tag{7}$$

where d is the cell thickness.

The dynamic equations for θ and ϕ_i may be written in bulk as

$$\gamma_\theta \frac{\partial \theta}{\partial t} = -\frac{\partial F}{\partial \theta} + \frac{\partial}{\partial y}\left(\frac{\partial F}{\partial(\partial \theta/\partial y)} \right), \tag{8}$$

$$\gamma_\phi \frac{\partial \phi_i}{\partial t} = -\frac{\partial F}{\partial \phi_i} + \frac{\partial}{\partial y}\left(\frac{\partial F}{\partial(\partial \phi_i/\partial y)} \right) \qquad (i=\mathrm{o} \text{ and e}), \tag{9}$$

where γ_θ and γ_ϕ are the viscosity coefficients for the $\mathbf{a}$ and $\mathbf{c}_i$, recpectively. While γ_θ must vanish for $\theta_0=\pi/2$, γ_ϕ should vanish for $\theta_0=0$. Therefore, from a symmetry consideration, we may expect the following relation between γ_θ and γ_ϕ as

$$\frac{\gamma_\phi}{\gamma_\theta} = \tan^2 \theta_0 \approx \theta_0^2 \qquad (\theta_0 \ll 1). \tag{10}$$

Hence the layer relaxation of the layer dynamics may be expected to be slower by a factor of 10–10^2 than that of the $\mathbf{c}$ director.

Then the torque balance equations at the boundaries are obtained as

$$\frac{\partial F}{\partial(\partial \phi_i/\partial y)} = \frac{\partial f_s^0}{\partial \phi_i} \qquad (y=0), \tag{11 a}$$

and

$$\frac{\partial F}{\partial(\partial \phi_i/\partial y)} = -\frac{\partial f_s^d}{\partial \phi_i} \qquad (y=d). \tag{11 b}$$

Finally the Poisson equation to determine φ can be derived as

$$\frac{\partial}{\partial y}\left\{ \varepsilon_{yy}(\theta, \phi_o, \phi_e)\left(\frac{\partial \varphi}{\partial y} \right) \right\} = P_s \frac{\partial}{\partial y}\left(\sum_i \cos\theta \cos\phi_i \right), \tag{12}$$

where the right-hand side corresponds to the polarization charge previously investigated in the surface-stabilized geometry [22–25]. Since the existence of the polarization charge increases the electrostatic energy, the apparent elastic constant seems to increase as the spontaneous polarization becomes large [22–25].

In the present work, we shall assume that $C=D=0$ and $\varepsilon_{yy}=$ constant for simplicity. Then defining the following effective elastic constants $K(\theta, \phi_o, \phi_e)$ for convenience

$$K(\theta, \phi_o, \phi_e) = A \sec^4 \theta + B \sum_i \sin^2 \phi_i, \tag{13}$$

the time evolution equations for θ and ϕ_i are derived as

$$\gamma_\theta \frac{\partial\theta}{\partial t} = K\frac{\partial^2\theta}{\partial y^2} + \frac{1}{2}\left(\frac{\partial K}{\partial\theta}\right)\left(\frac{\partial\theta}{\partial y}\right)^2 + \sum_i\left(\frac{\partial K}{\partial\phi_i}\right)\left(\frac{\partial\phi_i}{\partial y}\right)\left(\frac{\partial\theta}{\partial y}\right)$$
$$+ P_S\left(\frac{\partial\varphi}{\partial y}\right)\sum_i\cos\theta\sin\phi_i - 2L(\sec^2\theta - \sec^2\theta_0)\sec^3\theta\sin\theta \qquad (14)$$

and

$$\gamma_\phi\frac{\partial\phi_i}{\partial t} = B\frac{\partial^2\phi_i}{\partial y^2} - \frac{1}{2}\left(\frac{\partial K}{\partial\phi_i}\right)\left(\frac{\partial\theta}{\partial y}\right)^2 + P_S\left(\frac{\partial\varphi}{\partial y}\right)\cos\theta\sin\phi_i + K_p P_S^2(\delta_{io} - \delta_{ie})\sin(\phi_o - \phi_e) \qquad (15)$$

where

$$\frac{\partial K}{\partial\theta} = 4A\sec^5\theta\sin\theta, \qquad (16)$$

and

$$\frac{\partial K}{\partial\phi_i} = 2B\sin\phi_i\cos\phi_i. \qquad (17)$$

Then the torque balance equation at the boundaries is obtained as [22]

$$B\frac{\partial\phi_i}{\partial y} = \pm\tfrac{1}{4}\sigma g\left[\sin(\phi_i - \phi_0)\exp\left\{-\sigma\sin^2\left(\frac{\phi_i - \phi_0)}{2}\right)\right\} - \sin(\phi_i + \phi_0)\right.$$
$$\left.\times\exp\left\{-\sigma\cos^2\left(\frac{(\phi_i + \phi_0)}{2}\right)\right\}\right] \qquad (18)$$

where + and − are for $y=0$ and $y=d$, respectively, ϕ_0 is put into ϕ_0^0 and ϕ_0^d for $y=0$ and $y=d$, respectively [21].

Finally the Poisson equation reads

$$\frac{\partial}{\partial y}\left\{-\varepsilon_{yy}\left(\frac{\partial\varphi}{\partial y}\right) + P_S\sum_i\cos\theta\cos\phi_i\right\} = 0. \qquad (19)$$

Integrating this once, one has

$$-\varepsilon_{yy}\left(\frac{\partial\varphi}{\partial y}\right) + P_S\sum_i\cos\theta\cos\phi_i = D_y(t), \qquad (20)$$

where $D_y(t)$ is the electric displacement which was introduced as an integration constant and may depend on time. Assuming that ε_{yy} is a constant, for simplicity and similarly to previous work [24], and integrating equation (20) with respect to y again, one finds

$$-\varepsilon_{yy}\left(\frac{\varphi(d,t) - \varphi(0,t)}{d}\right) + P_S\frac{1}{d}\int_0^d dy\sum_i\cos\theta\cos\phi_i = D_y(t). \qquad (21)$$

From equations (20) and (21), we eventually have the internal electric field $E_y(y,t)$ in bulk as

$$E_y(y,t)=\frac{\left\{D_y(t)-P_S\sum_i \cos\theta\cos\phi_i\right\}}{\varepsilon_{yy}},$$

$$=-\frac{\partial\varphi}{\partial y}=E_{ex}+\frac{P_S}{\varepsilon_{yy}}\sum_i\{\langle\cos\theta\cos\phi_i\rangle-\cos\theta\cos\phi_i\}, \tag{22}$$

where

$$E_{ex}(t)=-\frac{\varphi(d,t)-\varphi(0,t)}{d}, \tag{23}$$

and

$$\langle\cos\theta\cos\phi_i\rangle=\frac{1}{d}\int_0^d dy\cos\theta\cos\phi_i. \tag{24}$$

In equation (22) E_{ex} corresponds to the externally applied electric field and the second term corresponds to the polarization electric field due to the spatial change of the polarization vector [22–24]. In fact if $P_S\cos\theta\cos\phi_i$ is constant through the sample, i.e. $\langle\cos\theta\cos\phi_i\rangle=\cos\theta\cos\phi_i$. For practical numerical computations, it is convenient to express the above-mentioned basic equations expressed in terms of some reduced variables.

$$r\frac{\partial\theta}{\partial\tau}=\kappa\frac{\partial^2\theta}{\partial\eta^2}+\frac{1}{2}\left(\frac{\partial\kappa}{\partial\theta}\right)\left(\frac{\partial\theta}{\partial\eta}\right)^2+\sum_i\left(\frac{\partial\kappa}{\partial\phi_i}\right)\left(\frac{\partial\phi_i}{\partial\eta}\right)\left(\frac{\partial\theta}{\partial\eta}\right)-e(\eta,\tau)\sum_i\sin\theta\cos\phi_i$$
$$-2\lambda(\sec^2\theta-\sec^2\theta_0)\sec^3\theta\sin\theta, \tag{25}$$

$$\frac{\partial\phi_i}{\partial\tau}=\frac{\partial^2\phi_i}{\partial\eta^2}-\frac{1}{2}\left(\frac{\partial\kappa}{\partial\phi_i}\right)\left(\frac{\partial\theta}{\partial\eta}\right)^2-e(\eta,\tau)\cos\theta\sin\phi_i+\gamma(\delta_{io}-\delta_{ie})\sin(\phi_o-\phi_e), \tag{26}$$

where

$$\tau=\left(\frac{B}{\eta_\phi d^2}\right)t, \tag{27}$$

$$\eta=\frac{y}{d}, \tag{28}$$

$$r=\frac{\eta_\theta}{\eta_\phi}, \tag{29}$$

$$\lambda=\frac{Ld^2}{B}, \tag{30}$$

$$\gamma=\frac{K_p(P_Sd)^2}{B}, \tag{31}$$

$$e(\eta,\tau)=\left(\frac{P_sd^2}{B}\right)E_y(y,t)=e_{ex}(\tau)+\Lambda\sum_i(\langle\cos\theta\cos\phi_i\rangle-\cos\theta\cos\phi_i), \tag{32}$$

$$\kappa(\theta,\phi_o,\phi_e)=\frac{K(\theta,\phi_o,\phi_e)}{B}=\alpha\sec^4\theta+\sum_i\sin^2\phi_i, \tag{33}$$

and

$$e_{ex}(\tau)=\left(\frac{P_s d^2}{B}\right)E_{ex}(\tau), \tag{34}$$

$$\langle\cos\theta\cos\phi_i\rangle=\int_0^1 d\eta\cos\theta\cos\phi_i, \tag{35}$$

$$\Lambda=\frac{(P_s d)^2}{B\varepsilon_{yy}}, \tag{36}$$

$$\alpha=\frac{A}{B}. \tag{37}$$

Here the parameter Λ is regarded as a measure of the effect of the polarization electric field as previously investigated in detail [20, 22–24]. Finally equation (18) reads

$$\frac{\partial\phi_i}{\partial\eta}=\tfrac{1}{4}\sigma\Gamma\left[\sin(\phi_i-\phi_0^0)\exp\left\{-\sigma\sin^2\left(\frac{\phi_i-\phi_0^0}{2}\right)\right\}-\sin(\phi_i+\phi_0^0)\right.$$
$$\left.\times\exp\left\{-\sigma\cos^2\left(\frac{(\phi_i+\phi_0^0)}{2}\right)\right\}\right], \tag{38 a}$$

$$\frac{\partial\phi_i}{\partial\eta}=-\tfrac{1}{4}\sigma\Gamma\left[\sin(\phi_i-\phi_0^d)\exp\left\{-\sigma\sin^2\left(\frac{(\phi_i-\phi_0^d)}{2}\right)\right\}-\sin(\phi_i+\phi_0^d)\right.$$
$$\left.\times\exp\left\{-\sigma\cos^2\left(\frac{(\phi_i+\phi_0^d)}{2}\right)\right\}\right] \tag{38 b}$$

where the normalized anchoring strength Γ is defined by

$$\Gamma=\frac{gd}{B}. \tag{39}$$

Then the normalized polarization along the y axis p_y and the switching current i_p can be defined by

$$p_y=\frac{1}{2}\sum_i\langle\cos\theta\cos\phi_i\rangle, \tag{40}$$

and

$$i_p(\tau)=\frac{dp_y(\tau)}{d\tau}=\frac{1}{2}\sum_i\frac{d\langle\cos\theta\cos\phi_i\rangle}{d\tau}, \tag{41}$$

respectively. Finally from equation (22), the normalized polarization electric field $e_p(\eta,\tau)$ can be expressed as

$$\begin{aligned}e_p(\eta,\tau)&=e(\eta,\tau)-e_{ex}(\tau)\\&=\Lambda\sum_i(\langle\cos\theta\cos\phi_i\rangle-\cos\theta\cos\phi_i),\end{aligned} \tag{42}$$

where one may note that the polarization field effect is just proportional to Λ.

3. Numerical results

Let us present below some numerical results based on equations (25), (26) and (38). In this paper, we shall focus our interest on the effect of the electric field on the layer structure in an $S_{C_A}^*$ phase.

In the following computations, we shall set the externally applied electric field $e_{ex}(\tau)$ into a sinusoidal one, i.e.

$$e_{ex}(\tau)=e_m \sin(2\pi f\tau). \tag{43}$$

It should be noted here that ϕ_0 depends on the molecular tilt angle and the layer tilt angle and the layer tilt angle β (β^0 for $y=0, \beta^d$ for $y=d$) in the following way:

$$\sin(\phi_0^0+\phi_p^0)=\frac{\tan\beta^0}{\tan\theta_0}, \tag{44 a}$$

$$\sin(\phi_0^d+\phi_p^d)=\frac{\tan\beta^d}{\tan\theta_0}, \tag{44 b}$$

where ϕ_p^0 and ϕ_p^d are introduced as a pretilt angle of the **c** director with respect to the bounding plate in the surface-stabilized geometry at $y=0$ and $y=d$, respectively [18]. From equations (44 a) and (44 b) one may see that the leaning angle β^0 and β^d must be smaller than the molecular tilt angle θ_0.

The unknown material parameters were set into the equations as follows,

$$r=10, \tag{45 a}$$

$$\alpha=2, \tag{45 b}$$

$$\lambda=10^5, \tag{45 c}$$

$$\Lambda=5, \tag{45 d}$$

$$\Gamma=10, \tag{45 e}$$

$$\sigma=5, \tag{45 f}$$

$$\phi_p^0=\phi_p^d=0, \tag{45 g}$$

$$\beta^0=\beta^d \text{ or } \beta^0=-\beta^d, \tag{45 h}$$

$$e_m=5\times 10^3, \tag{45 i}$$

$$f=1, \tag{45 j}$$

$$\gamma=3\times 10^2. \tag{45 k}$$

Here an antiferroelectric phase is assumed with $\gamma>0$ [18]. $\beta^0=\beta^d$ and $\beta^0=-\beta^d$ correspond to an inclined layer structure and a chevron one, respectively. Since the ϕ_p^0 and ϕ_p^d are assumed to be 0 in the following computations, the **n** director must be parallel to the bounding plate. In the present work we assumed a symmetric anchoring function with the same functional form $f_S^0(\phi_i)$ and $f_S^d(\phi_i)$ at the two boundaries. Therefore the dynamic behaviours of the odd-numbered layers and the even-numbered ones are equivalent in the following numerical results.

In the present paper let us consider the following two cases

$$\beta^0=-\beta^d, \quad \phi_0^0+\pi=\phi_0^d, \tag{46 a}$$

$$\beta^0=\beta^d, \quad \phi_0^0=\phi_0^d, \tag{46 b}$$

which correspond to an antiparallel anchoring in a chevron state and to a parallel anchoring in an inclined state, respectively.

In figures 1 and 2 we shall show the equilibrium states for a chevron and an inclined layer structure with no external field, or $e_m = 0$, respectively. Therein the molecular tilt angle θ_0 was set to 0·4. Then the dynamic behaviours for these two cases are presented in figures 3 and 4, respectively, for a cycle of the sinusoidal external field as defined by equation (43). Therein (*a*), (*b*), (*c*), (*d*), and (*e*) correspond to $e_{ex}(\tau) = 0$, $+e_m$, 0, $-e_m$, and 0 in a time sequence per cycle, respectively. From these it is found that the dynamic behaviours are asymmetric for a chevron layer structure and symmetric for an inclined one.

4. Discussions and conclusions

In this work we have presented the dynamic equations to investigate bistable switching in the surface-stabilized geometry. From a few numerical results, we have

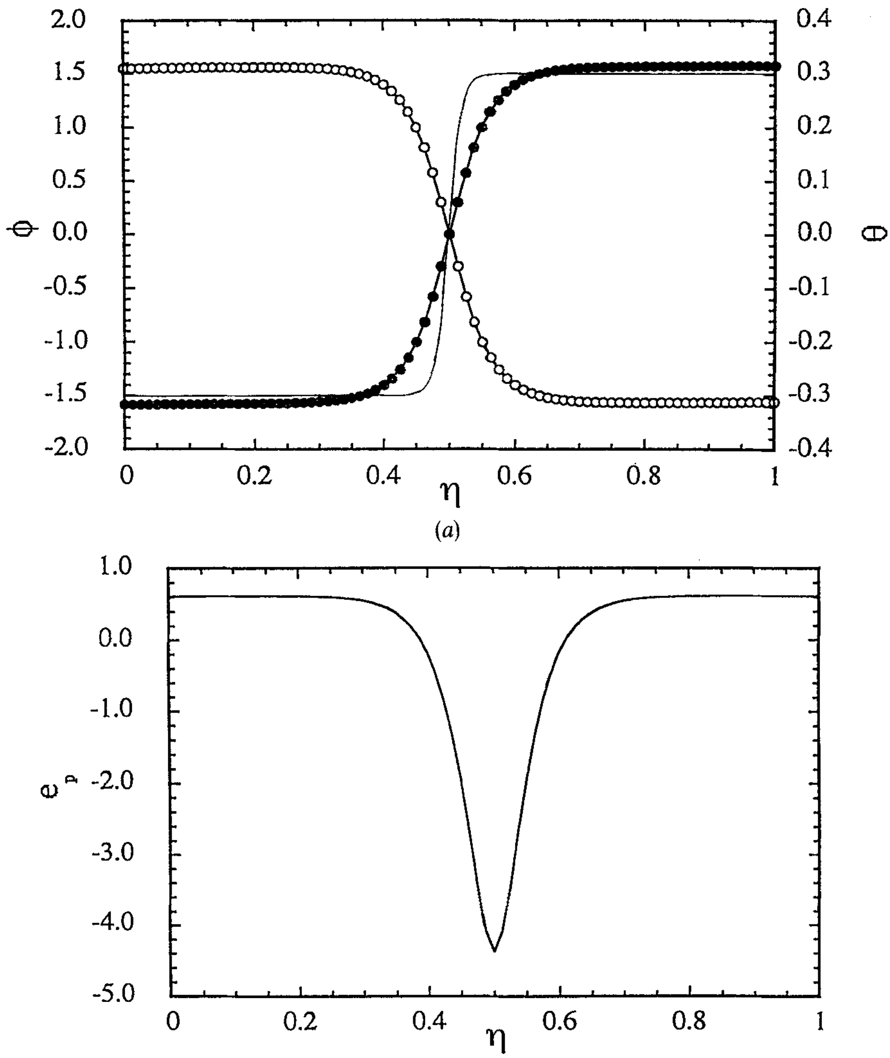

(*a*)

(*b*)

Figure 1. An equilibrium state for $\theta_0 = 0{\cdot}4$ and $\beta^u = -\beta^a = -0{\cdot}3$, or a chevron layer structure. Here ——, —○—, and —●— are for θ, ϕ_0 and ϕ_e, respectively. (*a*) θ, ϕ_0 and ϕ_e plotted with respect to y and (*b*) e_p plotted with respect to y.

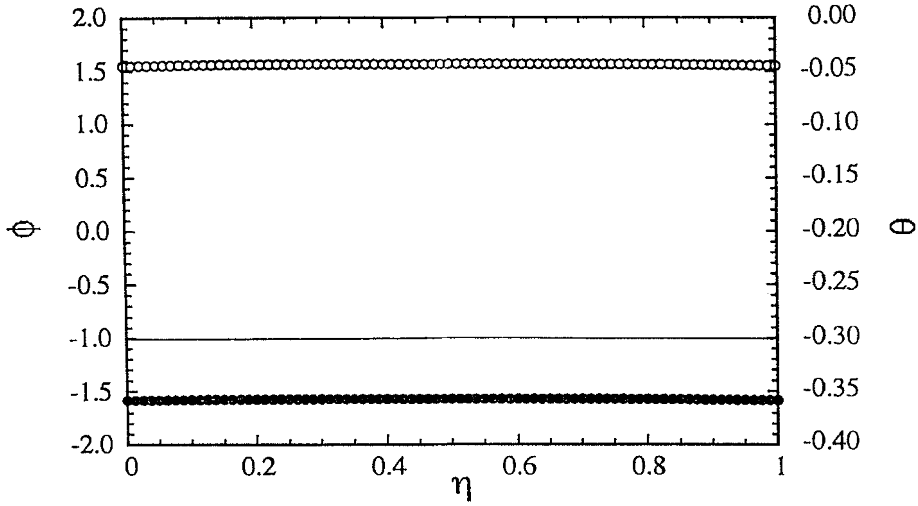

(*a*)

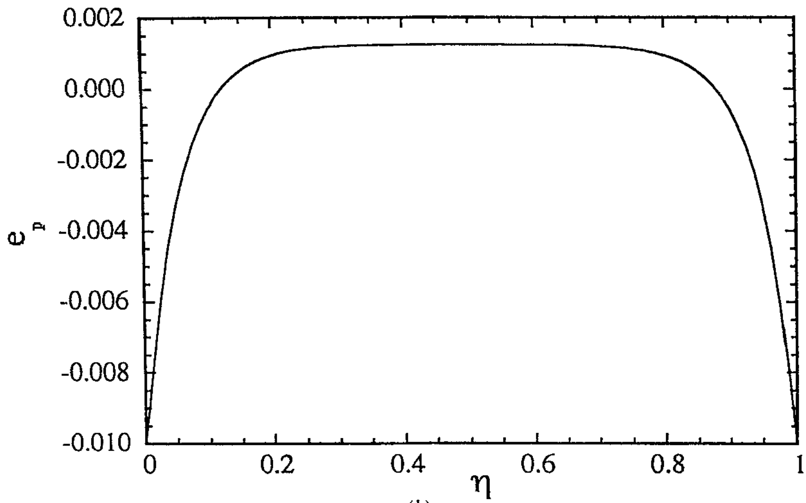

(*b*)

Figure 2. An equilibrium state for $\theta_0 = 0{\cdot}4$ and $\beta^0 = \beta^d = -0{\cdot}3$, or an inclined layer structure. Here ——, —○—, and —●— are for θ, ϕ_0 and ϕ_e, respectively. (*a*) θ, ϕ_0 and ϕ_e plotted with respect to y and (*b*) e_p plotted with respect to y.

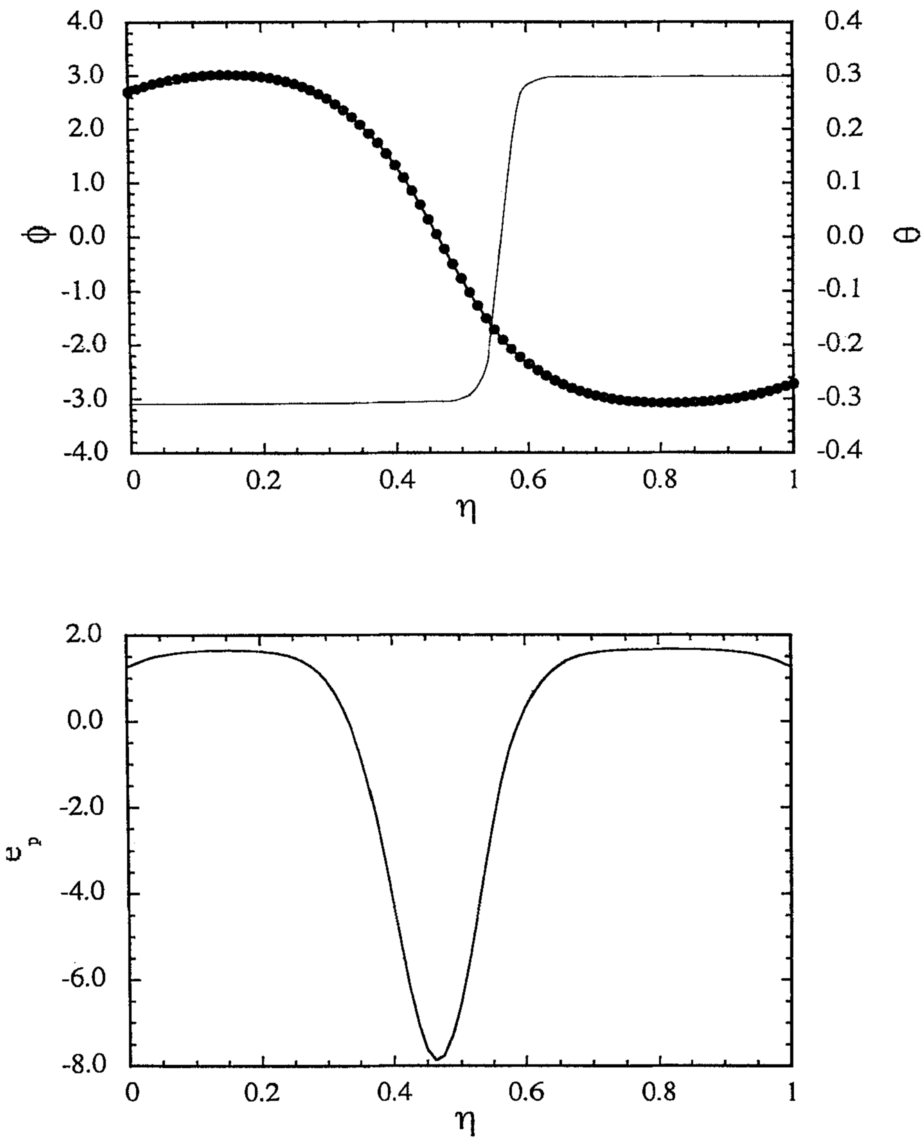
4.0
3.0
2.0
1.0
0.0
-1.0
-2.0
-3.0
-4.0
φ
0.4
0.3
0.2
0.1
0.0
-0.1
-0.2
-0.3
-0.4
θ
0
0.2
0.4
0.6
0.8
1
η
2.0
0.0
-2.0
-4.0
-6.0
-8.0
0
0.2
0.4
0.6
0.8
1
η

(a_2)

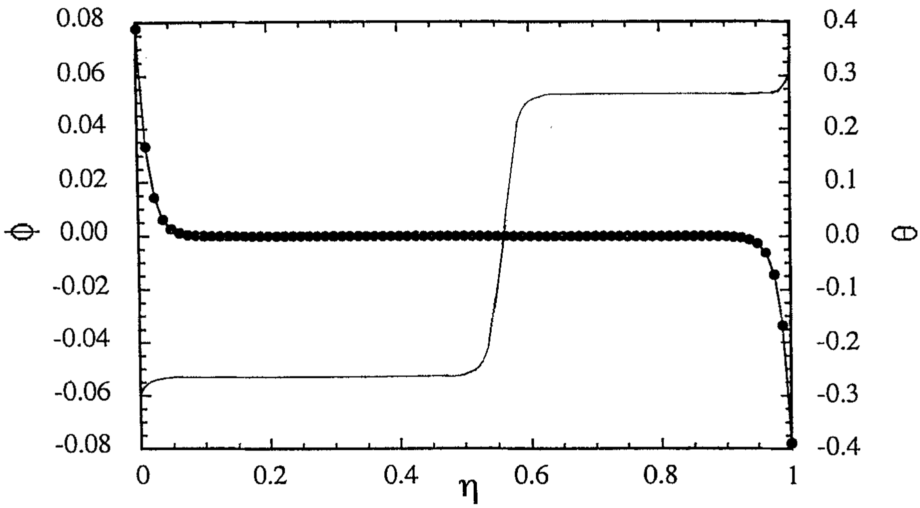
0.08
0.06
0.04
0.02
φ
0.00
-0.02
-0.04
-0.06
-0.08
0.4
0.3
0.2
0.1
0.0
θ
-0.1
-0.2
-0.3
-0.4
0
0.2
0.4
η
0.6
0.8
1

(b_1)

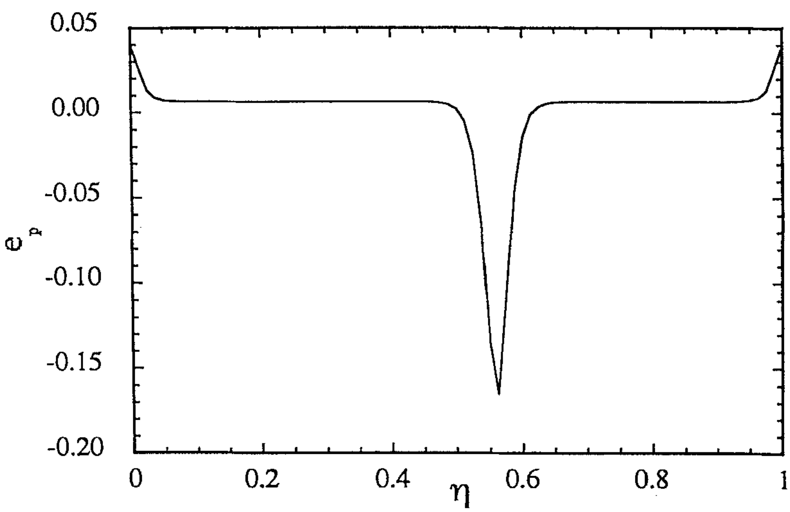
0.05
0.00
-0.05
e_p
-0.10
-0.15
-0.20
0
0.2
0.4
η
0.6
0.8
1

(b_2)

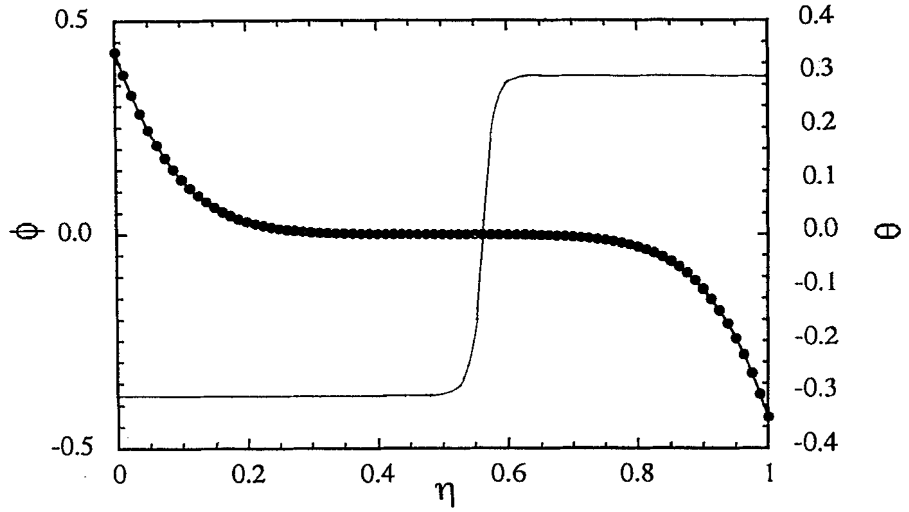
0.5
0.0
-0.5
φ
0.4
0.3
0.2
0.1
0.0
-0.1
-0.2
-0.3
-0.4
θ
0
0.2
0.4
0.6
0.8
1
η

(c_1)

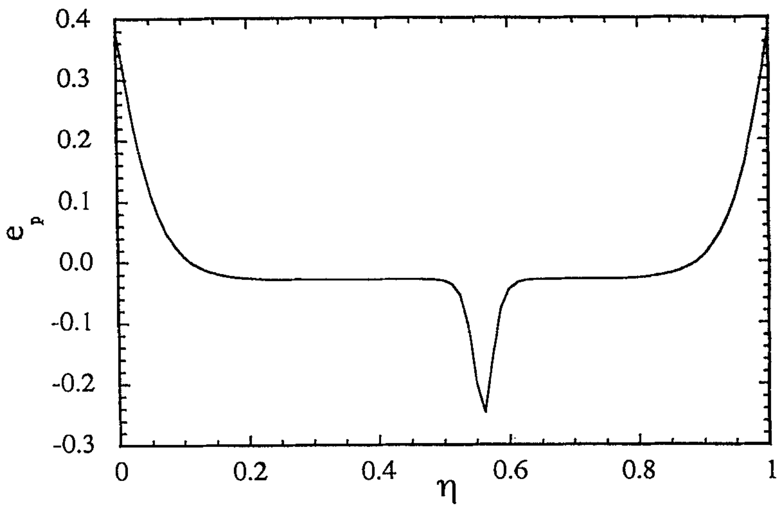
0.4
0.3
0.2
0.1
0.0
-0.1
-0.2
-0.3
e
p
0
0.2
0.4
0.6
0.8
1
η

(c_2)

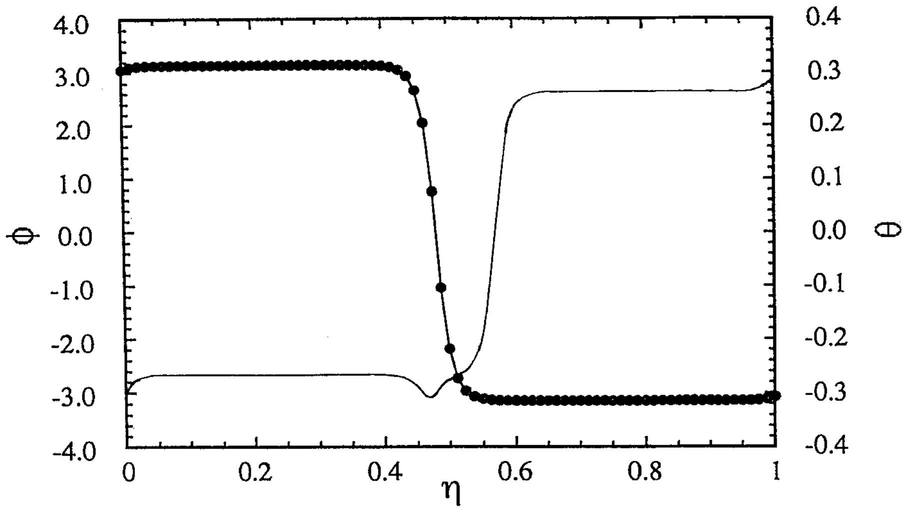
4.0
3.0
2.0
1.0
0.0
-1.0
-2.0
-3.0
-4.0
φ
0.4
0.3
0.2
0.1
0.0
-0.1
-0.2
-0.3
-0.4
θ
0
0.2
0.4
0.6
0.8
1
η

(d_1)

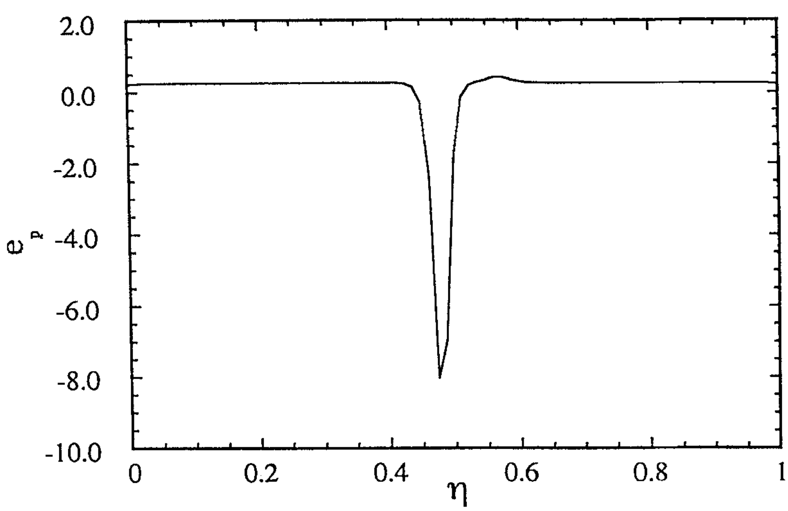
2.0
0.0
-2.0
-4.0
-6.0
-8.0
-10.0
e_p
0
0.2
0.4
0.6
0.8
1
η

(d_2)

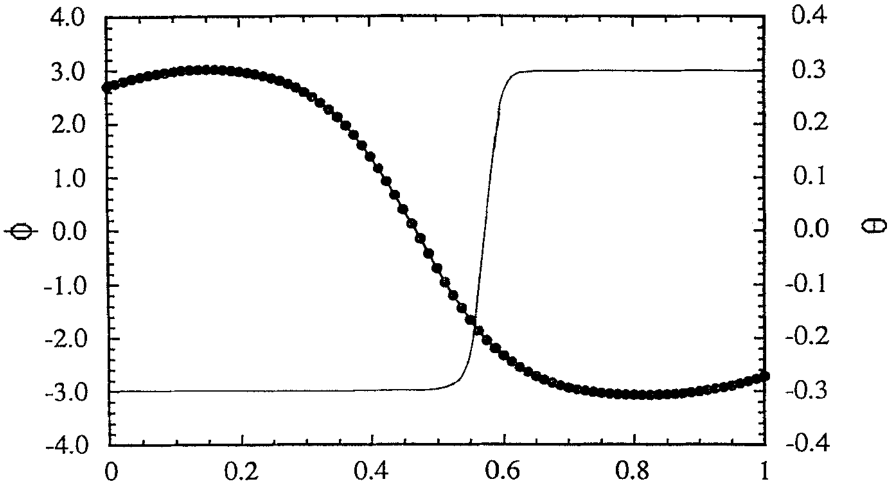

(e_1)

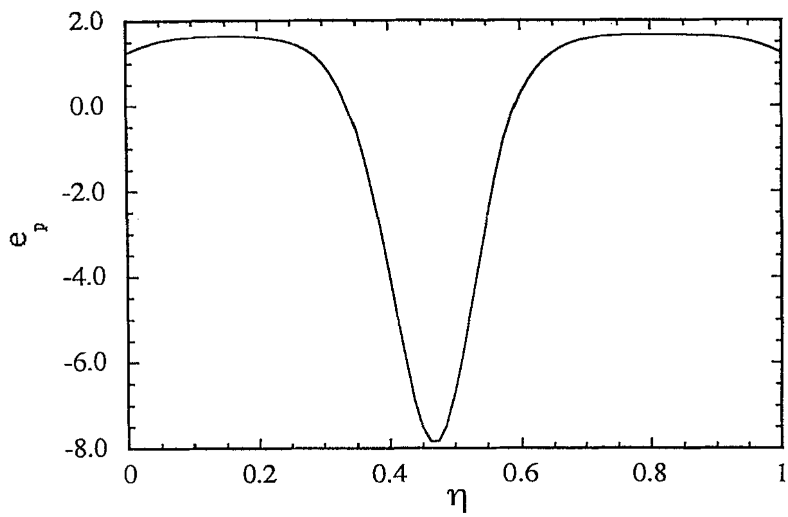

(e_2)

Figure 3. The dynamics in a cycle for $\theta_0 = 0{\cdot}4$ and $\beta^0 = -\beta^d = -0{\cdot}3$. (*a*) $e_{ex}(\tau) = 0$, (*b*) $e_{ex}(\tau) = +e_m$, (*c*) $e_{ex}(\tau) = 0$, (*d*) $e_{ex}(\tau) = -e_m$ and (*e*) $e_{ex}(\tau) = 0$. Here, in sub-set a_1, b_1, c_1, ——, and —●— are for θ, ϕ_0 and ϕ_e, respectively. In sub-set a_2, b_2, c_2 e_p is plotted with respect to y.

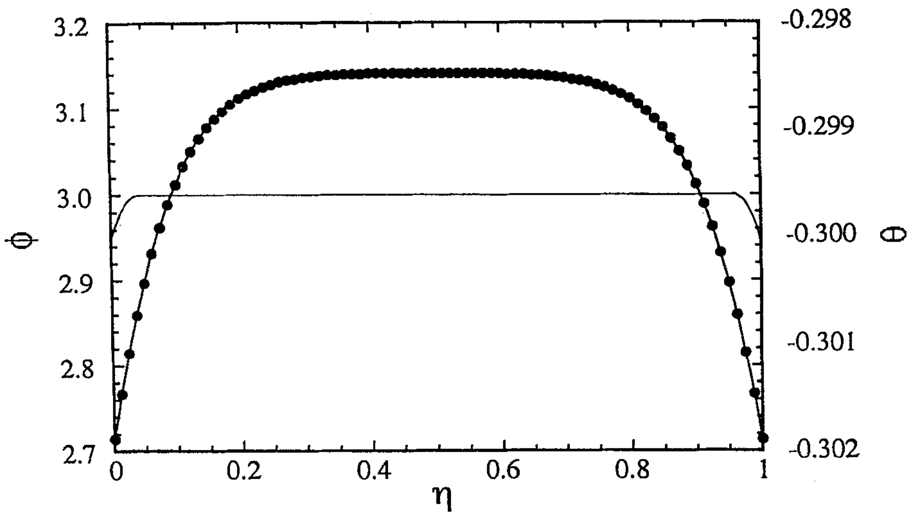
3.2
3.1
3.0
2.9
2.8
2.7
φ
-0.298
-0.299
-0.300
-0.301
-0.302
θ
0
0.2
0.4
0.6
0.8
1
η

(a_1)

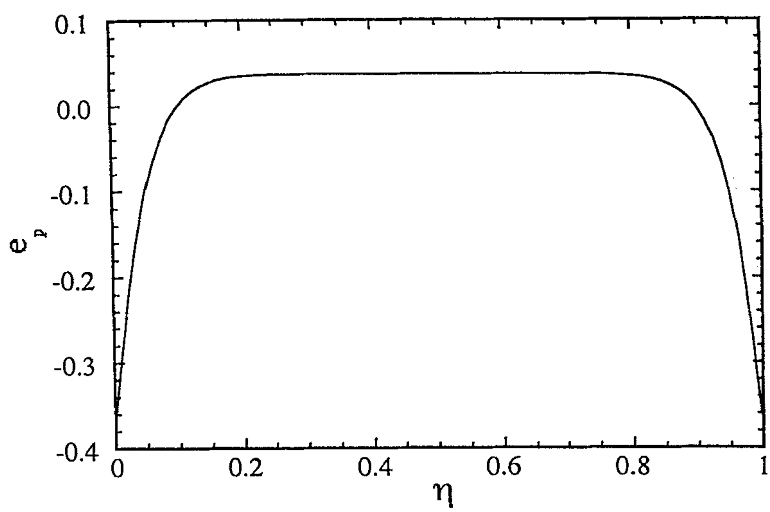
0.1
0.0
-0.1
-0.2
-0.3
-0.4
e_p
0
0.2
0.4
0.6
0.8
1
η

(a_2)

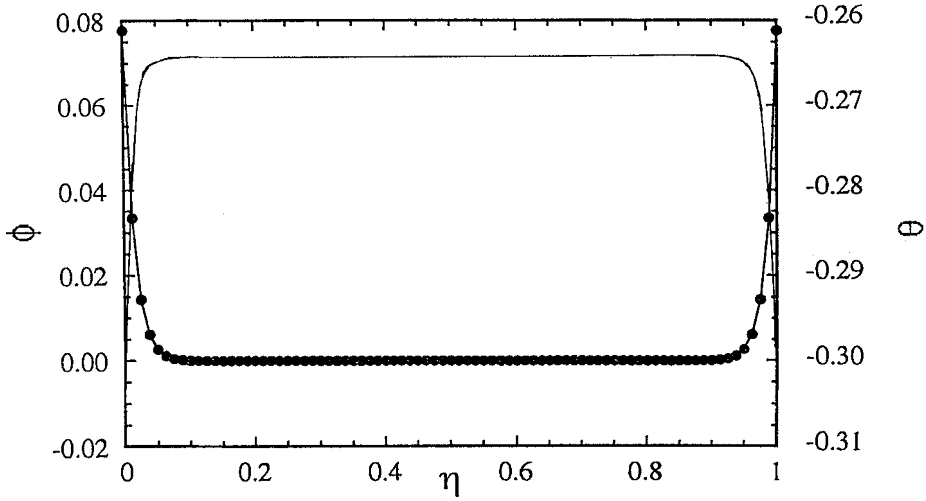
0.08
0.06
0.04
0.02
0.00
-0.02
φ
-0.26
-0.27
-0.28
-0.29
-0.30
-0.31
θ
0
0.2
0.4
η
0.6
0.8
1

(b_1)

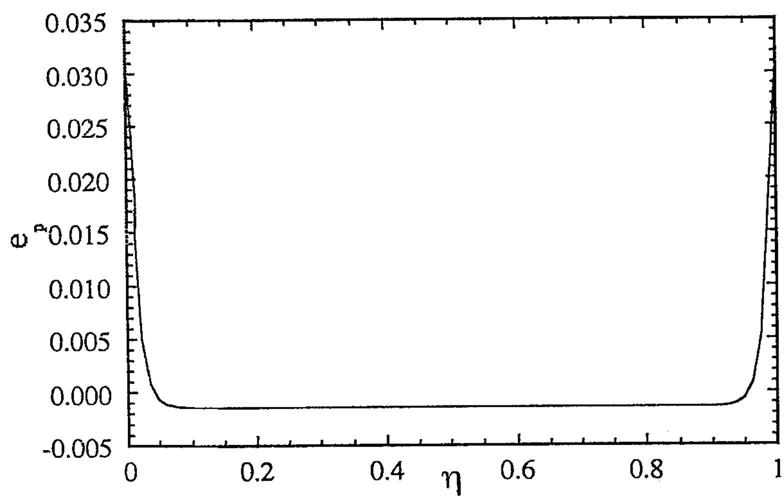
0.035
0.030
0.025
0.020
0.015
0.010
0.005
0.000
-0.005
e_p
0
0.2
0.4
η
0.6
0.8
1

(b_2)

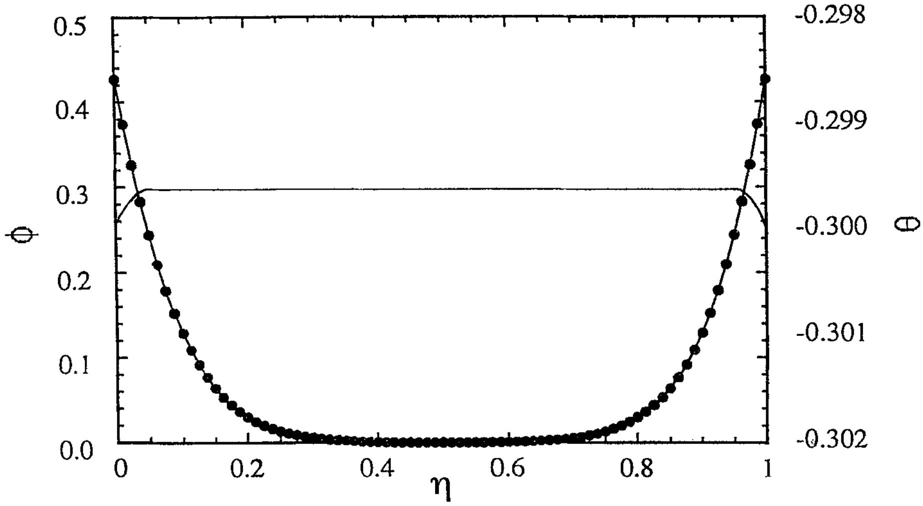
0.5
0.4
0.3
0.2
0.1
0.0
ϕ
-0.298
-0.299
-0.300
-0.301
-0.302
θ
0
0.2
0.4
0.6
0.8
1
η

(c_1)

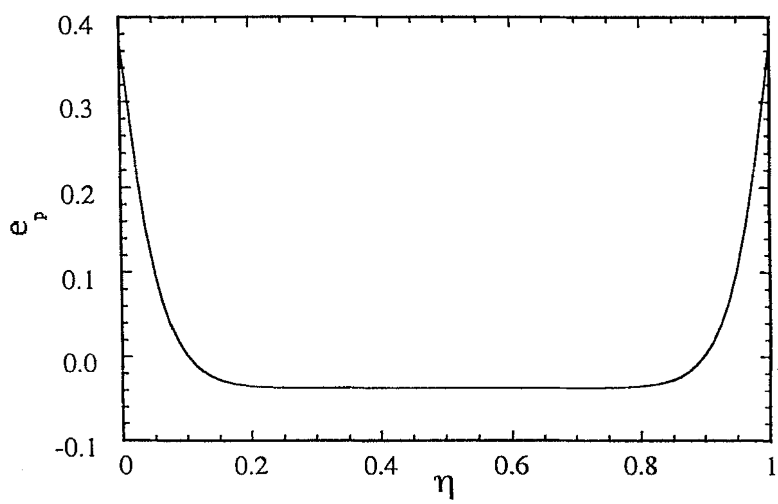
0.4
0.3
0.2
0.1
0.0
-0.1
e_p
0
0.2
0.4
0.6
0.8
1
η

(c_2)

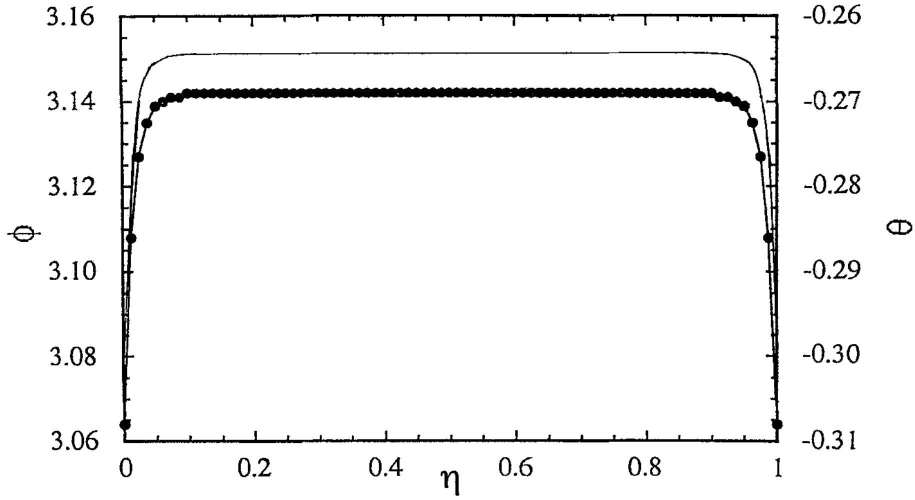
3.16
3.14
3.12
3.10
3.08
3.06
φ
-0.26
-0.27
-0.28
-0.29
-0.30
-0.31
θ
0
0.2
0.4
0.6
0.8
1
η

(d_1)

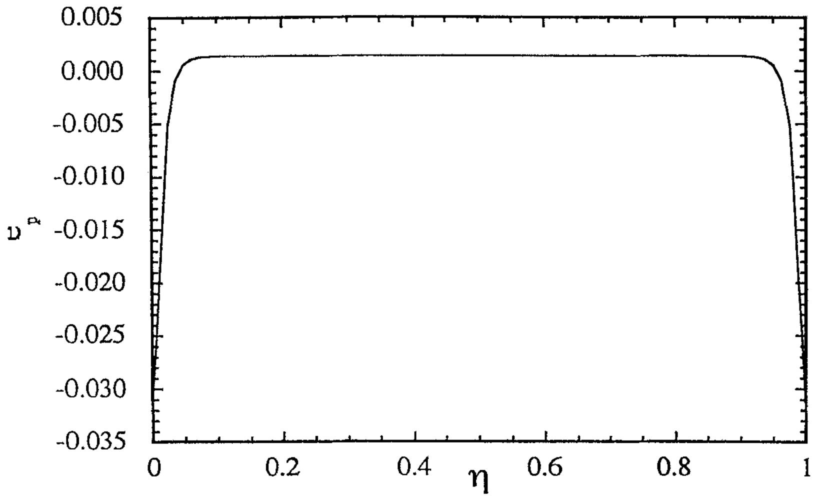
0.005
0.000
-0.005
-0.010
-0.015
-0.020
-0.025
-0.030
-0.035
0
0.2
0.4
0.6
0.8
1
η

(d_2)

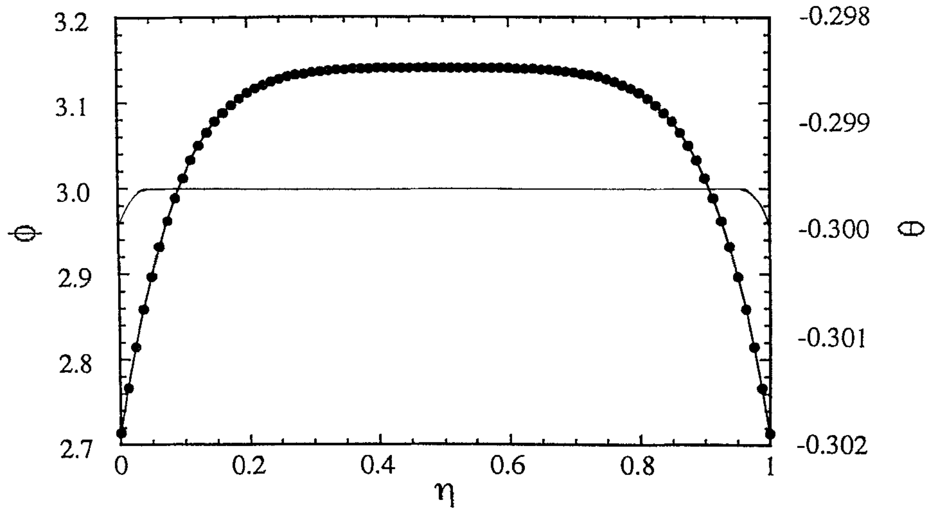

(e_1)

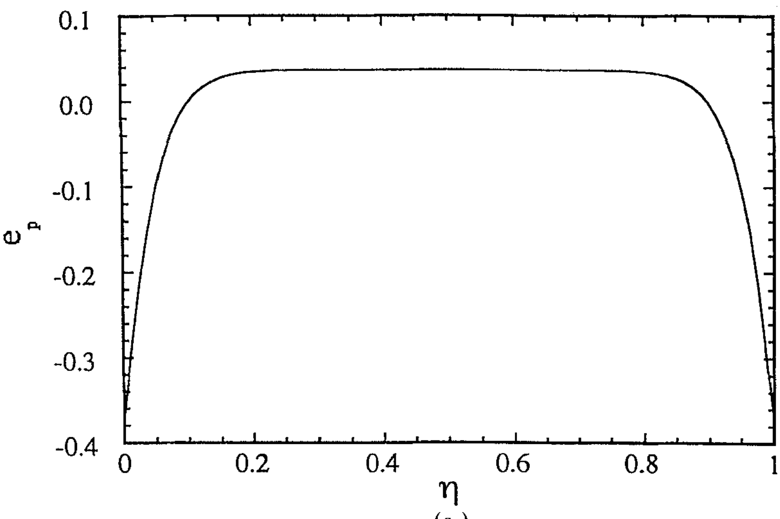

(e_2)

Figure 4. The dynamics in a cycle for $\theta_0 = 0{\cdot}4$ and $\beta^0 = \beta^d = -0{\cdot}3$. (*a*) $e_{ex}(\tau) = 0$, (*b*) $e_{ex}(\tau) = +e_m$, (*c*) $e_{ex}(\tau) = 0$, (*d*) $e_{ex}(\tau) = -e_m$ and (*e*) $e_{ex}(\tau) = 0$. Here, in sub-set a_1, b_1, c_1, ——, and —●— are for θ, ϕ_0 and ϕ_e, respectively. In sub-set a_2, b_2, c_2 e_p is plotted with respect to y.

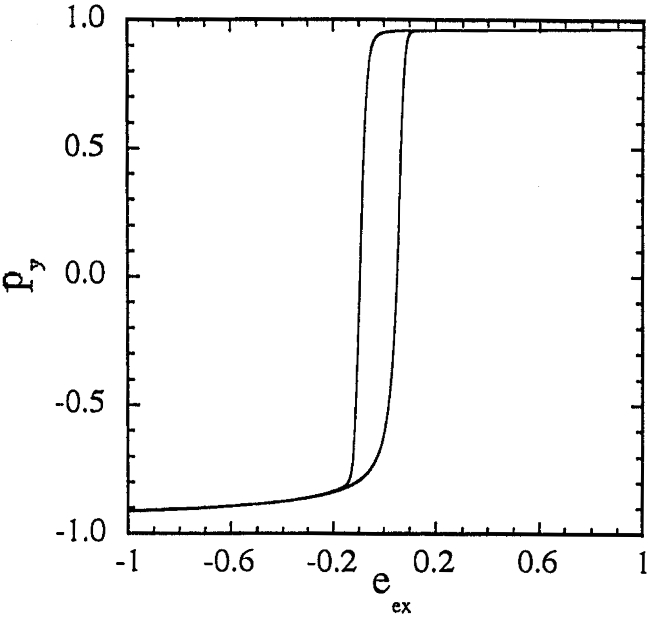

Figure 5. p_y–e_{ex} hysteresis loop for $\theta_0 = 0{\cdot}4$ and $\beta^0 = -\beta^d = -0{\cdot}3$, or a chevron state.

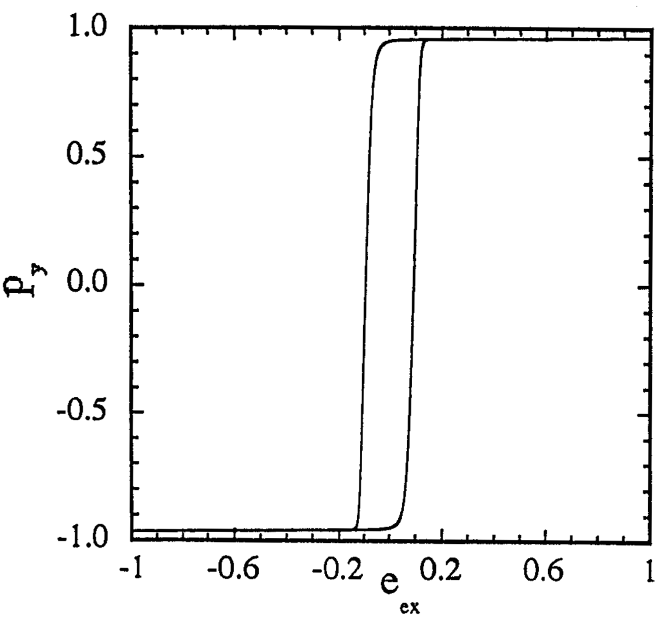

Figure 6. p_y–e_{ex} hysteresis loop for $\theta_0 = 0{\cdot}4$ and $\beta^0 = \beta^d = -0{\cdot}3$, or an inclined state.

found that an asymmetric bistable switching may be achieved in the chevron layers with an antiparallel anchoring which is consistent with the assumption such that the **n** director is parallel to the bounding plates at the boundaries. In practice, if we apply a sufficiently strong field to a chevron state in the surface-stabilized geometry, the **c** director may be accompanied by a disclination for the case that involves a large twist of the **c** director as shown in figure 2. On the other hand, for an inclined state, a symmetric dynamic behaviour was realized. Therefore from an application point of view for liquid crystal display devices, it seems to be important to obtain an inclined state rather than a chevron one.

At the end of this paper, we show hysteresis loops for the chevron and the inclined layers in figures 5 and 6, respectively. As might be expected from figures 2 and 3, the corresponding hysteresis loops are also found to be asymmetric and symmetric for the chevron and the inclined layers, respectively.

As a future problem, it seems to be worthwhile to investigate anchoring effects in dynamic responses under a pulsed external field in detail. Moreover, the previously reported hydrodynamic theory for an incompressible S_C [17] remains to be extended in the future to the case of the presently discussed compressible S_C^* liquid crystal layers.

References

[1] MEYER, R. B., LIEBERT, L., STRZELECKI, L., and KELLER, P., 1975, *J. Phys., France*, **36**, L69.
[2] MEYER, R. B., 1977, *Molec. Crystals liq. Crystals*, **40**, 33.
[3] CLARK, N. A., and LAGERWALL, S. T., 1980, *Appl. Phys. Lett.*, **36**, 899.
[4] BERESNEV, L. A., BLINOV, L. M., OSIPOV, M. A., and PIKIN, S. A., 1988, *Molec. Crystals liq. Crystals* A, **158**, 3.
[5] KLEMAN, M., 1983, *Points, Lines and Walls* (Wiley).
[6] ORSAY GROUP, 1971, *Solid St. Commun.*, **9**, 653.
[7] RAPINI, A., 1972, *Phys., France*, **33**, 237.
[8] DE GENNES, P. G., 1975, *The Physics of Liquid Crystals* (Oxford), Chap. 7.
[9] DAHL, I., and LAGERWALL, S. T. 1984, *Ferroelectrics*, **58**, 215.
[10] NAKAGAWA, M., 1990, *Liq. Crystals*, **8**, 651.
[11] NAKAGAWA, M., 1989, *Molec. Crystals liq. Crystals*, **174**, 65.
[12] NAKAGAWA, M., 1990, *Displays* (Butterworth), p. 67.
[13] NAKAGAWA, M., 1990, *J. phys. Soc. Jap.*, **59**, 1995.
[14] CLARK, N. A., and LAGERWALL, S. T., 1986, *Proc. 6th International Display Research Conference*, Tokyo, Japan, p. 456.
[15] RIEKER, T. R., CLARK, N. A., SMITH, G. S., PARMER, D. S., SIROTA, E. B., and SAFINIA, C. R., 1987, *Phys. Rev. Lett.*, **59**, 2658.
[16] OUCHI, Y., LEE., J., TAKEZOE, H., FUKUDA, A., KONDO, K., KITAMURA, T., and MUKOH, A., 1988, *Jap. J. appl. Phys.*, **27**, L725.
[17] LESLIE, F. M., STEWART, I. W., and NAKAGAWA, M., 1991, *Molec. Crystals liq. Crystals*, **198**, 443.
[18] NAKAGAWA, M., 1991, *Jap. J. appl. Phys.*, **30**, 1759.
[19] CHANDANI, A. D. L., HAGIWARA, H., SUZUKI, Y., OUCHI, Y., TAKEOZE, H., and FUKUDA, A., 1988, *Jap. J. appl. Phys.*, **27**, L729.
[20] NAKAGAWA, M., 1989, *J. phys. Soc. Jap.*, **58**, 2346.
[21] NAKAGAWA, M., 1991, *Ferroelectrics*, **122**, 279.
[22] NAKAGAWA, M., ISHIKAWA, M., and AKAHANE, T., 1988, *Jap. J. appl. Phys.*, **27**, 456.
[23] NAKAGAWA, M., and AKAHANE, J., 1986, *J. phys. Soc. Jap.*, **55**, 1516.
[24] NAKAGAWA, M., and AKAHANE, J., 1986, *J. phys. Soc. Jap.*, **55**, 4492.
[25] NAKAGAWA, M., 1989, *Molec. Crystals liq. Crystals*, **173**, 1.